CHAPTER 10

In silico investigation on the inhibition of $A\beta_{1-42}$ peptide aggregation by $A\beta_{1-40}$ peptide using potential of mean force study

In silico investigation on the inhibition of $A\beta_{1-42}$ peptide aggregation by $A\beta_{1-40}$ peptide using potential of mean force study

10.1. Abstract:

Recent experimental data revealed that small, soluble $A\beta_{1-42}$ peptide oligomers especially dimers impair synaptic plasticity and memory leading to AD. Here, we have studied dimerization of $A\beta_{1-42}/A\beta_{1-42}$ homo-dimer and $A\beta_{1-40}/A\beta_{1-42}$ hetero-dimer in terms of free energy profile by all-atom simulations using the ff99SB force field. We have found that in presence of $A\beta_{1-40}$ peptide, there exists a strong tendency to form a hetero-dimer with $A\beta_{1-42}$ peptide, suggesting that a possible co-oligomerization. Furthermore, we have investigated the effects of $A\beta_{1-40}$ on the $A\beta_{1-42}$ peptide. Our study also shows that in presence of $A\beta_{1-40}$ peptide, the β-content of $A\beta_{1-42}$ peptide is reduced. Additionally, certain residues important for bending in $A\beta_{1-42}$ peptide attained an increased flexibility in presence of $A\beta_{1-40}$ peptide. The salt-bridge destabilization also manifested the impact of $A\beta_{1-40}$ peptide on $A\beta_{1-42}$ peptide as a whole. Based on this, one may expect that $A\beta_{1-40}$ peptide inhibits the aggregation propensity of $A\beta_{1-42}$ peptide. Moreover, the binding free energy obtained by the MM-PBSA method also revealed a strong affinity between the two isoforms thereby suggesting that $A\beta_{1-40}$ peptide binding induces conformational change in $A\beta_{1-42}$ peptide. Our results suggest that co-oligomerization of Aβ peptide isoforms may play a substantial role in AD.

10.2. Introduction:

Recent experimental studies have reported that $A\beta_{1-40}$ peptide, in addition to its unique quality to assemble, also has the characteristic feature to inhibit protofibril and fibril formation of $A\beta_{1-42}$ peptide [233,234]. With progression of AD, the ratio of Aβ40:42 have been shown to decrease; despite the fact that expression of $A\beta_{1-40}$ peptide in AD brain is ten times greater than that of $A\beta_{1-42}$ peptide [235]. Regardless of the fact that, $A\beta_{1-40}$ peptide has been reported to decrease the toxicity of $A\beta_{1-42}$ peptide, lack of accurate molecular information by which both the isoform interact with each other complicates the therapeutic targets, impeding normal drug development approaches aimed at preventing neurodegeneration in AD. To better understand the mechanism by which $A\beta_{1-40}$ peptide interacts with $A\beta_{1-42}$ peptide and inhibits its toxicity, the protein-

protein interaction study is crucial. In this work we have applied a combinatorial approach comprising of MD simulation and US methodology [140] to study the interaction of $A\beta_{1-42}$ peptide in the presence and absence of $A\beta_{1-40}$ peptide. Moreover, the binding free energy ΔG_{bind} of $A\beta_{1-40}$ peptide to the receptor $A\beta_{1-42}$ peptide was calculated using the MM-PBSA method.

10.3. Materials & Methods:

10.3.1. Computational model of $A\beta_{1-42}/A\beta_{1-40}$ hetero-dimer and $A\beta_{1-42}/A\beta_{1-42}$ homo-dimer:

The initial monomer structure of $A\beta_{1-42}$ peptide and $A\beta_{1-40}$ peptide were retrieved from RCSB Protein Data Bank, PDB entries: 1IYT [211] and 2LFM [236], respectively. The monomeric structures were then solvated with TIP3P water model with solvent buffer being 10 Å in all directions individually [170]. To neutralize the negative charge Na+ ions close to the solute surface were added. Minimization, heating and equilibration was carried out as described in Chapter 5 (section 5.3.1).

The equilibrated monomeric structures after equilibration was used to generate the possible homo-dimer $A\beta_{1-42}/A\beta_{1-42}$ and hetero-dimer $A\beta_{1-42}/A\beta_{1-40}$ structures. Using the PatchDock [175] web server, the selected conformer of $A\beta_{1-42}$ peptide was docked to the copy of itself, and onto $A\beta_{1-40}$ peptide; the best energy homo-dimer and hetero-dimer were chosen, respectively in terms of minimum free energy and maximum contact surface area. The homo-dimer and hetero-dimer complex with the maximum atomic contact energy and minimum global energy were selected for further PMF [172] study as discussed in Chapter 5 (section 5.3.3). Each set of the simulations contains 20 and 18 simulation windows, respectively for $A\beta_{1-42}/A\beta_{1-40}$ hetero-dimer and $A\beta_{1-42}/A\beta_{1-42}$ homo-dimer; the RCs were extended 11 Å ($A\beta_{40}$) and 10 Å ($A\beta_{42}$) away from the initial distances.

10.3.2. Interface residues and hot spot residues identification:

The lowest energy conformer of the $A\beta_{1-42}/A\beta_{1-40}$ hetero-dimer was isolated from the PMF plot and MD simulation was carried on. Using the PDBsum server the interface residues and hot spot residues were analysed [180]. Interface residues are defined as the residues with a contact distance less than 6 Å from the interacting partner.

10.4. Results & Discussions:

10.4.1. Free energy profile:

One of the best ways to display the interaction between two proteins is by computing the free energy profile of their association. In this study, the interaction study of the $A\beta_{1-42}/A\beta_{1-40}$ hetero-dimer was performed using US simulations with distance as a function of time. **Figure 10.1** shows the result of the free energy profile.

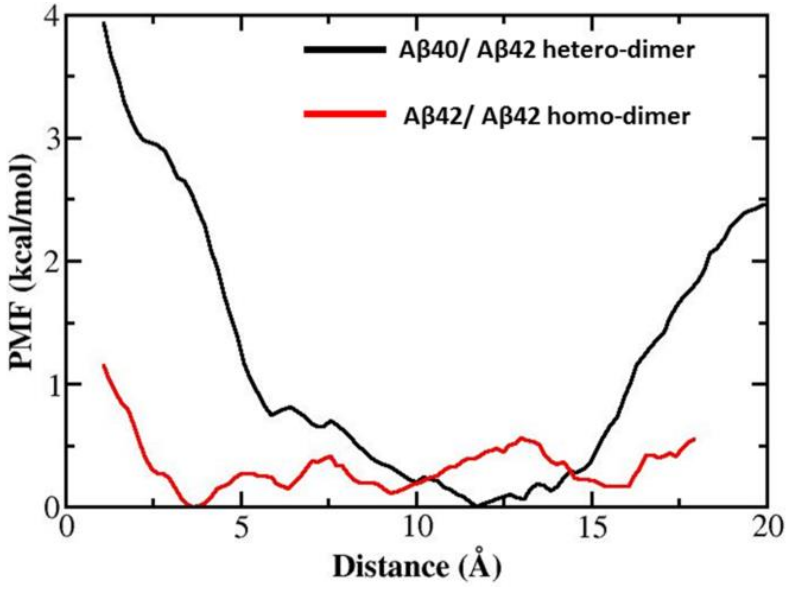

Figure 10.1. *Potential of mean force of $A\beta_{1-42}/A\beta_{1-40}$hetero-dimer and $A\beta_{1-42}/A\beta_{1-42}$ homo-dimer (in kcal/mol) as a function of the inter-chain distance (in Å) which is between the center of mass (COM) of the C-α atom of two monomers.*

In case of the $A\beta_{1-42}/A\beta_{1-42}$ homo-dimer complex, the two monomers tend to associate at a very close inter-chain distance of ~ 3 Å. Since $A\beta_{1-42}$ peptide aggregation is known to be a key risk factor for the onset and progress of AD, it is not surprising to get a distance of close proximity [237, 238]. But after a certain distance, the two monomers can easily get separated, as their dissociation energy is found to be quite low from the PMF plot.

Although the global minimum structure of $A\beta_{1-42}/A\beta_{1-40}$ hetero-dimer is formed around 13 Å distance, in contrary to $A\beta_{1-42}/A\beta_{1-42}$ homo-dimer, it exhibits higher dissociation energy of ~ 4kcal/mol indicating strong association between them. This is in accordance with previous studies that report the co-oligomer formation of $A\beta_{1-40}$ & $A\beta_{1-42}$ peptide [239]. This indicates that $A\beta_{1-42}$ peptides have a preference to bind to

$A\beta_{1-42}$ peptide over $A\beta_{1-40}$ peptide and therefore, high concentration of $A\beta_{1-40}$ peptide will be required to generate hetero-dimers.

10.4.2. Conformational dynamics of $A\beta_{1-42}/A\beta_{1-42}$ homo-dimer and $A\beta_{1-42}/A\beta_{1-40}$ hetero-dimer:

The conformational details of this study are further discussed. As shown in **Figure 10.2. A & B,** different conformations were observed for the $A\beta_{1-42}/A\beta_{1-42}$ homo-dimer and $A\beta_{1-42}/A\beta_{1-40}$ hetero-dimer at different inter-chain distances. From the conformational changes undergone by the $A\beta_{1-42}/A\beta_{1-42}$ homo-dimer, it can be clearly seen that after a certain distance of separation, the $A\beta_{1-42}$ monomer tends to dissociate from the other $A\beta_{1-42}$ monomer, (**Figure 10.2. A**) which leads to a lower dissociation energy as evident from the PMF graph of **Figure 10.1**. Also, the helical portion is reduced in both the monomeric units and the enhancement of random coil is more prominent in $A\beta_{1-42}/A\beta_{1-42}$ homo-dimer. Although β pleated sheets were not observed in the dimeric unit at different inter-chain distances, there is a probability of appearance of β-strands as helical content was reducing to coils.

This was further ascertained by the probability score graph wherein occurrence of β-strand are visible in both the increasing and decreasing inter-chain distances at the C-terminal region, respectively (**Figure 10.3. A & B**). On the other hand, in the presence of $A\beta_{1-40}$ peptide, the α-helical content of $A\beta_{1-42}$ peptide was restrained and both the monomeric unit was observed to remain in a close contact to each other which confirms their strong association to form the hetero-dimer (**Figure 10.2. B**).

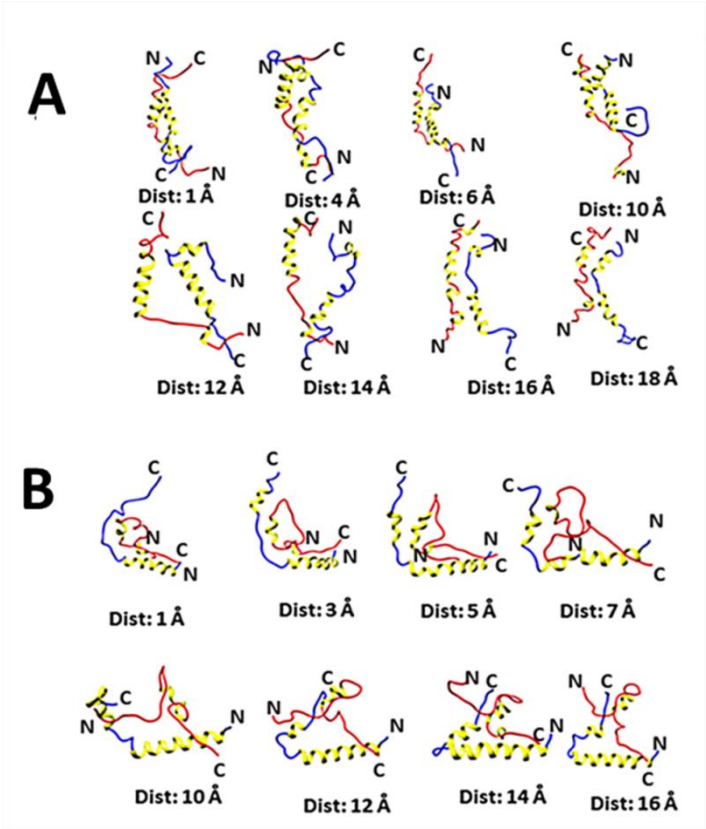

Figure 10.2. *A) Snapshots of the $A\beta_{1-42}/A\beta_{1-42}$ homo-dimer; B) snapshots of the $A\beta_{1-42}/A\beta_{1-40}$hetero-dimer at 300K during the time course of simulation period at varying inter-chain distances in Å.*

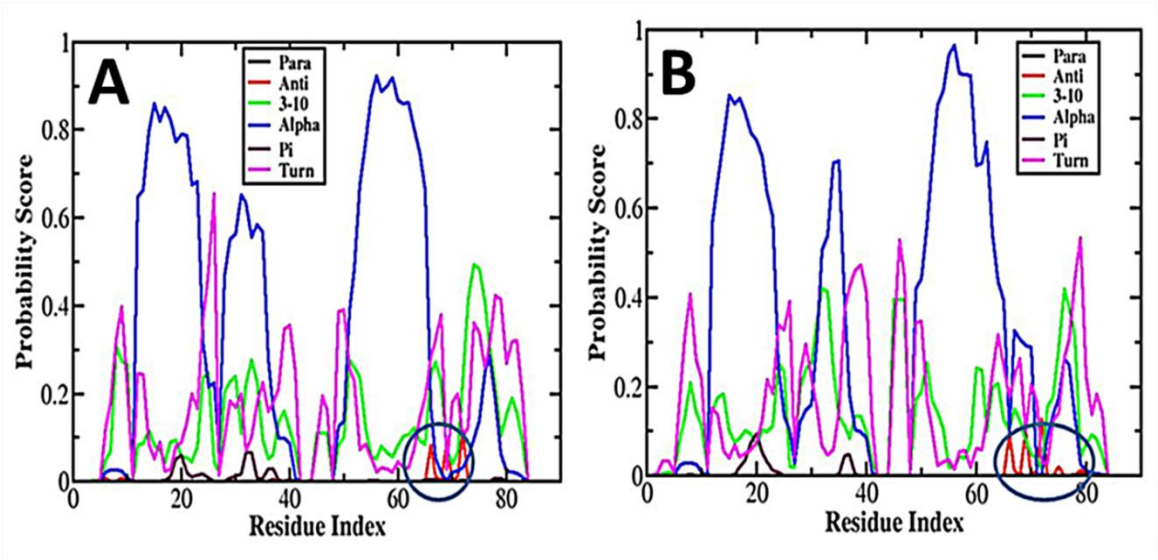

Figure 10.3. *Probability score of secondary structure assignment per residue for the average structure of $A\beta_{1-42}$ monomer of the $A\beta_{1-42}/A\beta_{1-42}$ homo-dimer taken from the molecular dynamics simulation trajectory: A) increasing inter-chain distance; B) decreasing inter-chain distance.*

This is in agreement with the probability score graph obtained from the DSSP tool (**Figure 10.4. A & B**). Both of the probability graphs (increased inter-chain distance and decreased inter-chain distance) show that the monomeric units displayed helices and coils in most of the regions. We can thus say that there is a strong tendency to form $A\beta_{1-42}/A\beta_{1-40}$ co-oligomer in suitable conditions. Consequently, it may be suggested that the underlying mechanism of inhibition might lie in the association of the two peptides thereby reducing the β-contents of $A\beta_{1-42}$ peptide. Our results are thus is in good agreement with the experimental results of Yang and Wang [240].

10.4.3. Hydrogen bonding analysis of $A\beta_{1-42}/A\beta_{1-40}$ hetero-dimer:

To shed light on the nature of ordering of the peptides in the hetero-dimer complex, we have studied the overall inter-molecular and intra-molecular hydrogen bonds of the $A\beta_{1-42}/A\beta_{1-40}$ hetero-dimer that play a vital role in stabilizing the dimerization process. To calculate the hydrogen bonds, the cut off for angle and distance was set to 120^0 and 3.5 Å, respectively. **Figure 10.5.A** show the total number of hydrogen bonds between the two monomers, wherein two distinct cases were considered: $A\beta_{1-42}$ peptide as an acceptor and monomer $A\beta_{1-40}$ as a donor followed by $A\beta_{1-40}$ as a donor and $A\beta_{1-42}$ as an acceptor. The total number of inter-molecular hydrogen bond was found to be around 10. **Figure 10.5.B** shows the total number of hydrogen bonds among the residues of each monomer separately and the total number of intra-molecular hydrogen bonds was found to be in the range of ~17. Thus hydrogen bonding proves to be crucially important in stabilizing the hetero-dimer complex.

10.4.4. Conformational dynamics of the lowest energy conformer of the $A\beta_{1-40}/A\beta_{1-42}$ hetero-dimer and $A\beta_{1-42}/A\beta_{1-42}$ homo-dimer using distance restraints:

The global minima structure of the $A\beta_{1-42}/A\beta_{1-40}$ hetero-dimer and $A\beta_{1-42}/A\beta_{1-42}$ homo-dimer was isolated and further simulation was carried out with constant distance restraint up to 20 ns. On the basis of energetics, this lowest energy structure is found to represent the most probable hetero-dimer structure that may have formed. Hence, further studies on this structure will shed lights on important aspects that will be helpful in the understanding of the actual dimerization process. The conformational dynamics of the global minima structure of the $A\beta_{1-42}/A\beta_{1-40}$ hetero-dimer shows strong

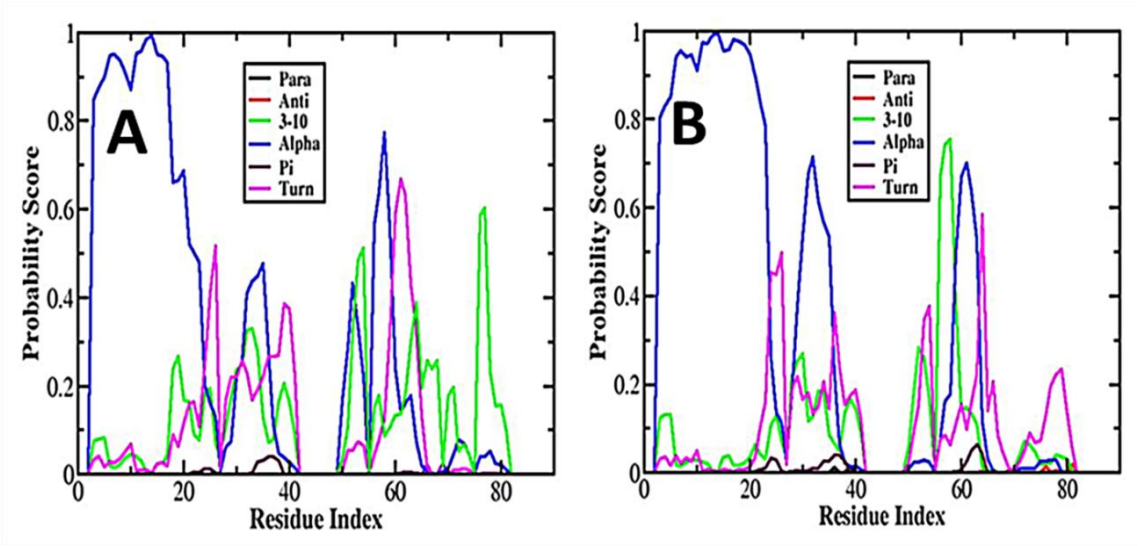

Figure 10.4. *Probability score of secondary structure assignment per residue for the average structure of $A\beta_{1-42}$ monomer of the $A\beta_{1-42}/A\beta_{1-40}$ hetero-dimer taken from the molecular dynamics simulation trajectory A) increasing inter-chain distance; B) decreasing inter-chain distance.*

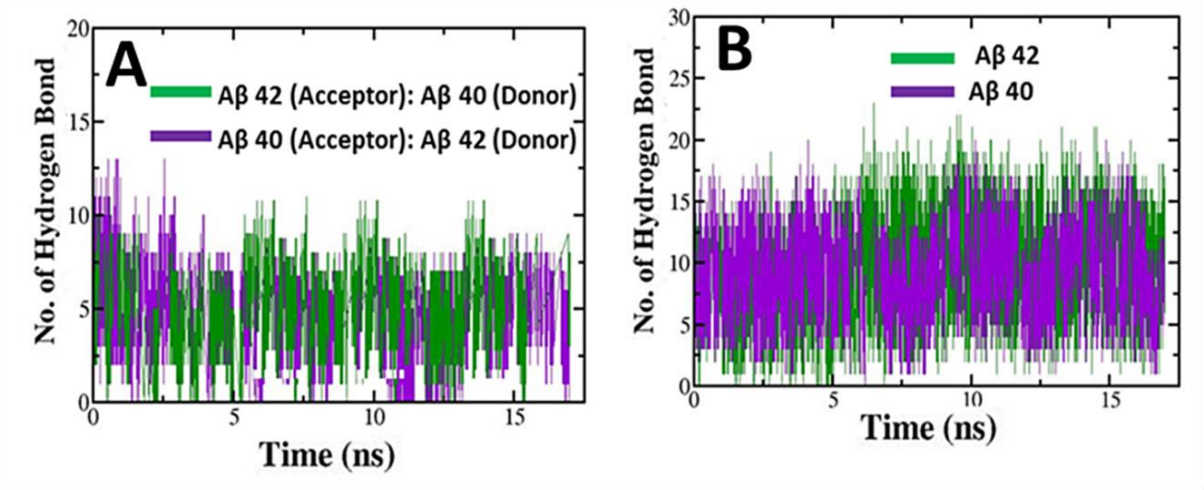

Figure 10.5. *Total number of: A) inter-molecular hydrogen bonds; B) intra-molecular hydrogen bonds as a function of time for the $A\beta_{1-42}/A\beta_{1-40}$ hetero-dimer at constant inter-chain distance.*

association between the two isoforms indicating a higher probability to form co-oligomers (**Figure 10.6**). From the snapshots, it can be clearly seen that Aβ $_{1-42}$ peptide tends to stay in its native conformation with maximum helical contents.

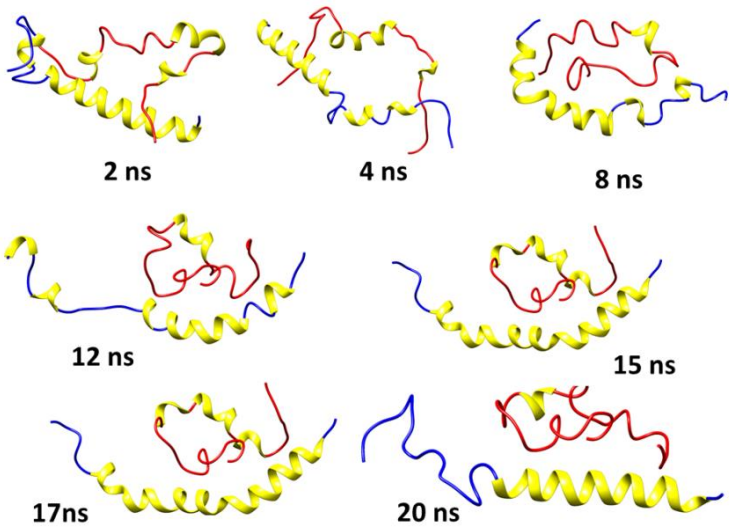

***Figure 10.6**. Snapshots of $A\beta_{1-42}/A\beta_{1-40}$ hetero-dimer obtained after MD simulation run at constant inter-chain distance (13 Å).*

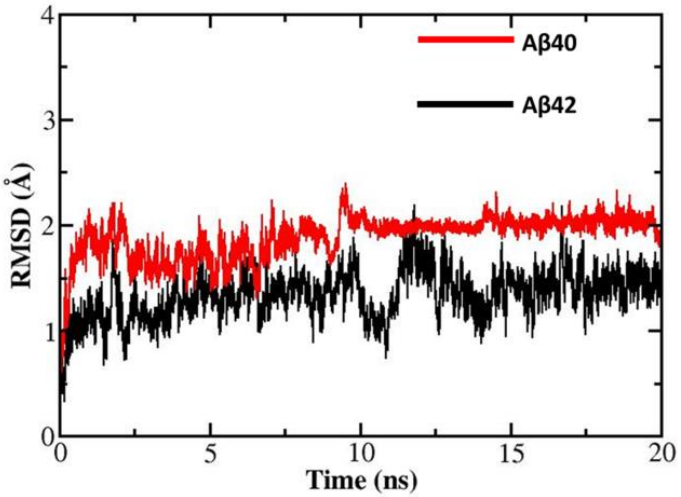

***Figure 10.7.** Backbone RMSD vs time course of simulation period for the $A\beta_{1-42}/A\beta_{1-40}$ hetero-dimer complex at the constant distance.*

To monitor the stability and flexibility of the $A\beta_{1-42}/A\beta_{1-40}$ hetero-dimer, the RMSDs of the C-α atoms from their initial position were analyzed from the trajectories of the global minima structure that was run at constant distance. As shown in **Figure 10.7**, the simulated $A\beta_{1-42}/A\beta_{1-40}$ hetero-dimer achieved stability after about 2.5 ns. In addition, more deviation, as a whole, is displayed in $A\beta_{1-40}$ monomer than $A\beta_{1-42}$ monomer.

It can be thus inferred that in the presence of $A\beta_{1-40}$ peptide, the $A\beta_{1-42}$ peptide attains its stability. Although it may contradict the common sense that $A\beta_{42}/A\beta_{40}$ hetero-dimer complex formation can restrict the deviation of the $A\beta_{1-40}$ peptide to a larger extent because of the stronger protein-protein interactions, the increased deviation can be explained by the fact that the $A\beta_{1-40}$ monomer might have undergone conformational changes to accommodate each other and reach the optimal binding mode (induced-fit phenomenon), and thus the binding process showed amplified deviations.

The root-mean-square fluctuations (RMSFs) of the $A\beta_{1-42}$ peptide in presence of $A\beta_{1-40}$ peptide were subsequently calculated. Residues encompassing the region 18-33 were found to be more flexible in $A\beta_{1-42}$ peptide (**Figure 10.8**). As previous studies have reported the formation of bent structure within residues 22-28 to be significant in the fibril formation [241, 242], thus accelerated flexibility of these regions specifies that $A\beta_{1-40}$ has the capacity to inhibit the $A\beta_{1-42}$ fibril formation.

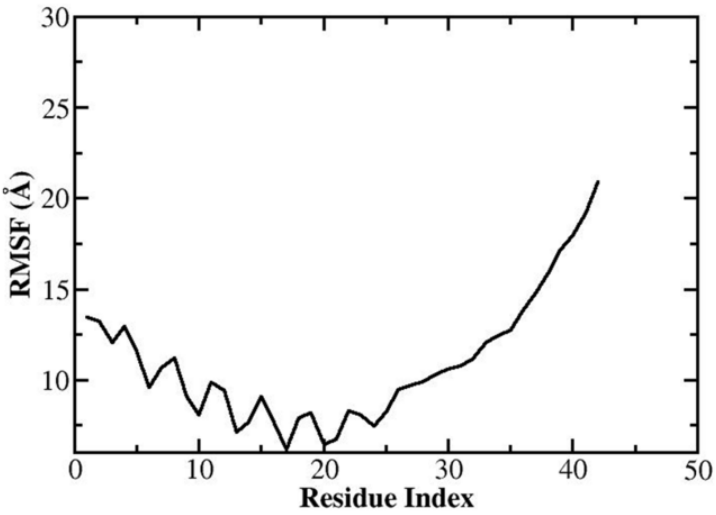

Figure 10.8. *RMSF of C-α atoms for each residue using the backbone atomic fluctuation as a function of amino acids for the lowest energy conformer $A\beta_{1-42}/A\beta_{1-40}$ hetero-dimer.*

Furthermore, the total energy and potential energy for the global minima structure of the $A\beta_{1-42}/A\beta_{1-40}$ hetero-dimer at constant distance was analyzed. **Figure 10.9** shows the total energy to have a negative value thereby confirming the stability of the $A\beta_{1-42}/A\beta_{1-40}$ hetero-dimer structure. As observed from the **Figure 10.9**, a higher negative value for potential energy was perceived, which is indicative of a greater stability in the protein structure.

In accordance with its inhibitory mechanism, we studied the effect of $A\beta_{1-40}$ peptide on dynamics of the salt bridge of $A\beta_{1-42}$ peptide. As evident from the time dependence and distributions as shown in **Figure 10.10. A**, distance between Asp23 & Lys28 of $A\beta_{1-42}$ is larger in presence of $A\beta_{1-40}$ than in homo-dimer state. In the case of homo-dimer, we have the measured the distance between Asp23 & Lys28 to be 4 Å (**Figure 10.10. B**), while for hetero-dimer it is ~8 Å. So it can be said that $A\beta_{1-40}$ peptide is likely to exhibit its subsidiary inhibitory effect by increasing the distance between residue Asp23 & Lys28 that form the salt bridge which is known to play an important role in stabilizing the turn region [194]. Thus by destabilizing the salt-bridge, $A\beta_{1-40}$ peptide can inhibit the aggregation propensity of $A\beta_{1-42}$ peptide.

10.4.5. Protein-Protein interaction study:

In order to study the interactions between the monomers of homo-dimer and hetero-dimer, we analyzed the global minimum structures which form the most stable complex with the minimum free energy respectively.

i) Interactions in homo dimer: We have isolated those lowest energy conformers and carried out the protein-protein interaction studies in the PDBsum server [180]. **Figure 9.11.A** shows the residues involved in the homo-dimer formation. In case of $A\beta_{1-42}/A\beta_{1-42}$ homo-dimer most of the C-terminal regions were found to get involved in the association process. The interface area for each monomer was found to be around ~ 900 $Å^2$ as shown in **Figure 10.11.B.** The numbers of bonded and non-bonded contacts involved were apparently found to be 91 non-bonded contacts, 2 hydrogen bonds and 1 salt bridge.

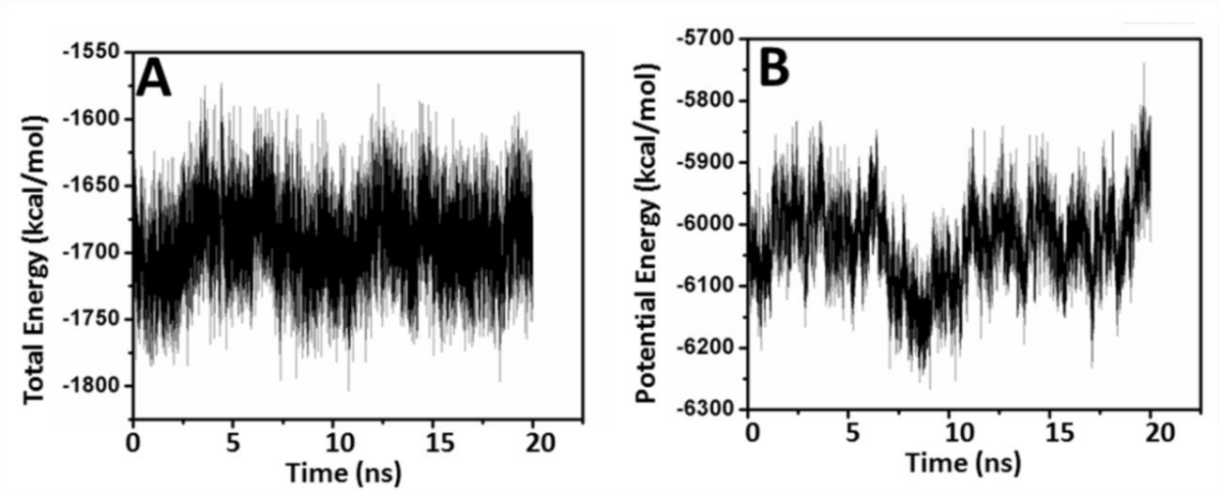

Figure 10.9. *A) Total Energy; B) Potential Energy vs time course of simulation period for the $A\beta_{1-42}/A\beta_{1-40}$ hetero-dimer at constant inter-chain distance.*

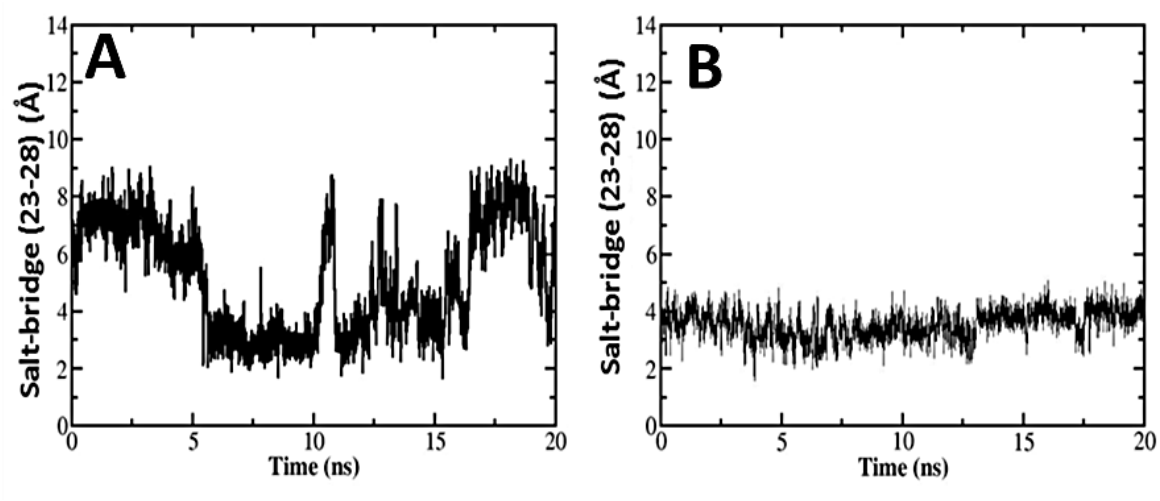

Figure 10.10. *Time dependence distance between Asp23 and Lys28 of: A) lowest energy conformer $A\beta_{1-42}/A\beta_{1-40}$ hetero-dimer; B) lowest energy conformer $A\beta_{1-42}/A\beta_{1-42}$ homo-dimer.*

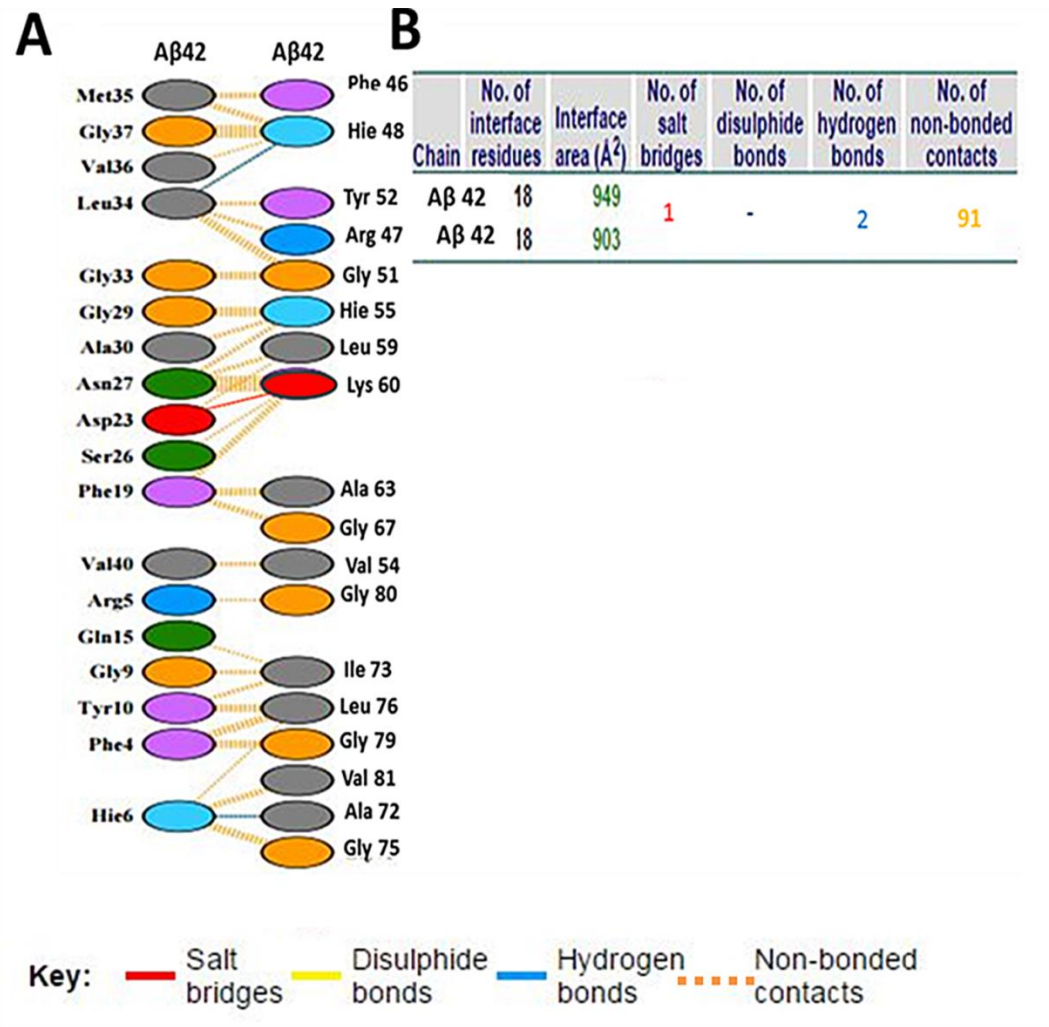

Figure 10.11. *A) The interface residues; B) The interface plot statistics of lowest energy conformer of $A\beta_{1\text{-}42}/A\beta_{1\text{-}42}$ homo-dimer at constant distance.*

ii) Interactions in hetero-dimer: Different interactions that play a crucial role in the hetero-dimer association are shown in **Figure 10.12**. As shown in **Figure 10.12.A**, a large number of non-bonded contacts, 12 hydrogen bonds and 3 salt bridges were found to aid in the association of the two isoforms. The N-terminal region is found to be involved in the interactions between the two isoform to form the hetero-dimer. So, we can say that the N-terminal region of $A\beta_{1\text{-}42}$ peptide is important for the co-oligomer formation. Numbers of interface residues involved in the hetero-dimer formation were found to be ~19 and the interface area for each monomeric unit was fund to be in the range of ~900 $Å^2$ as shown in **Figure 10.12. B**. This concurs with the above mentioned overall hydrogen bond analysis, wherein the inter-peptide hydrogen bond number appears to be approximately the same with the inter-molecular hydrogen bonds present in the lowest energy conformer. The non-bonded contacts between the two monomeric

units bring the monomeric units together, allowing the backbone-backbone interactions of the dimer to initiate the dimer formation.

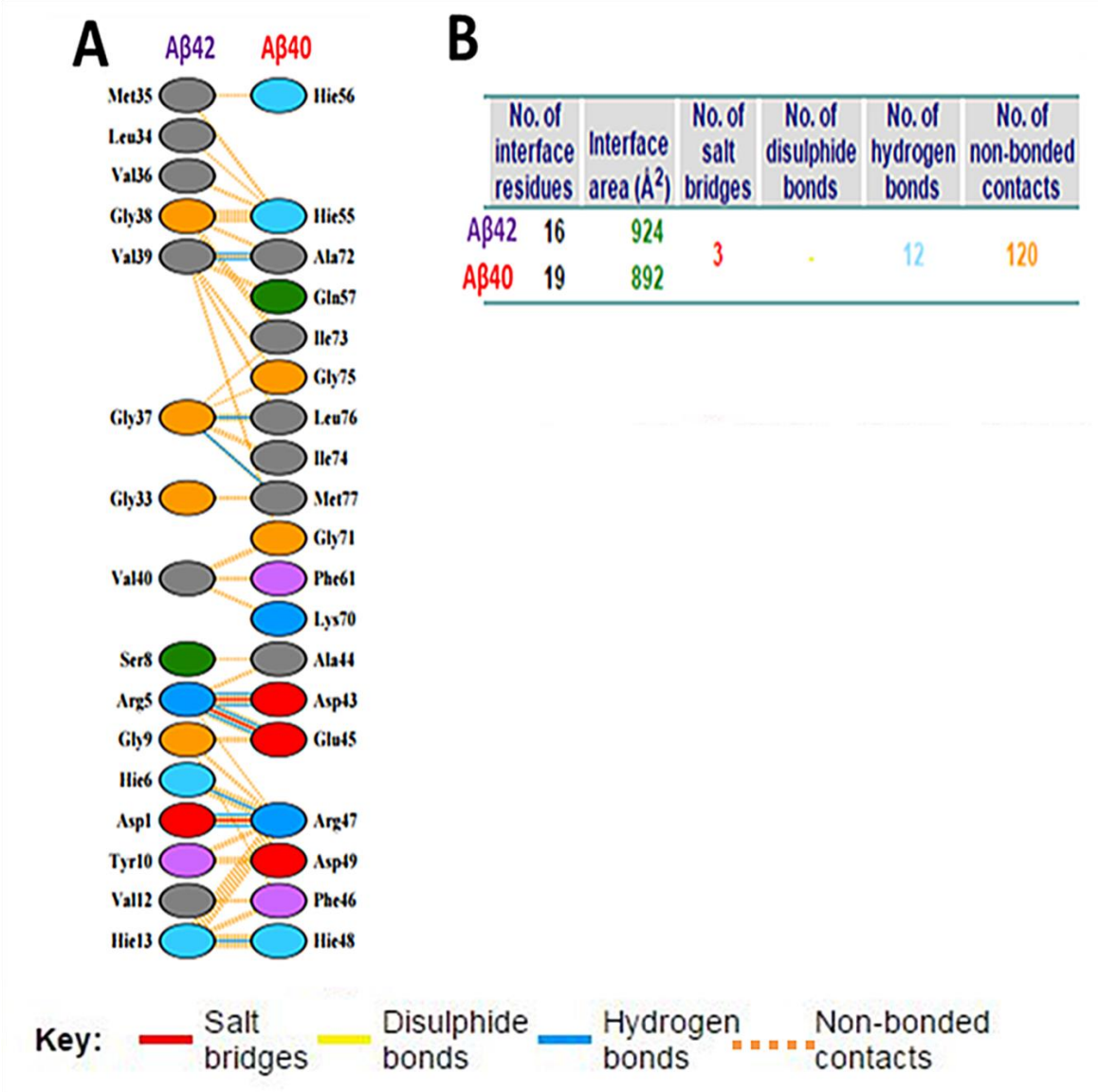

Figure 10.12.*A) The interface residues of lowest energy conformer $A\beta_{1\text{-}42}/A\beta_{1\text{-}40}$ hetero-dimer; B) The interface plot statistics of the lowest energy conformer $A\beta_{1\text{-}42}/A\beta_{1\text{-}40}$ hetero-dimer at constant distance.*

Although three salt bridge formations were found to stabilize the hetero-dimer formation, the Asp23-Lys28 salt bridge that is known to be very important in the self-aggregation of $A\beta_{1-42}$ peptide was not formed when we separately studied the protein-protein interaction of the $A\beta_{1-42}$ peptide that was pulled out from the hetero-dimer complex (**Figure 10.13**). It is in good agreement with the result obtained from **Figure 10.11,** emphasizing the impact of $A\beta_{1-40}$ peptide on the salt-bridge of $A\beta_{1-42}$ peptide.

The binding energetics between the $A\beta_{1-42}$ peptide and the $A\beta_{1-40}$ peptide in terms of *van der Waals* forces and electrostatic interactions were also calculated (**Figure 10.14.A & B**). The specificity of interaction between the $A\beta_{1-42}$ peptide and the $A\beta_{1-40}$ peptide being manifested on both the electrostatic energy and the *van der Waals* forces formed the basis of the aforementioned calculations. Both the electrostatic energy and the *van der Waals* energy displayed higher negative values suggesting strong favourable interactions between the $A\beta_{1-42}$ peptide and the $A\beta_{1-40}$ peptide.

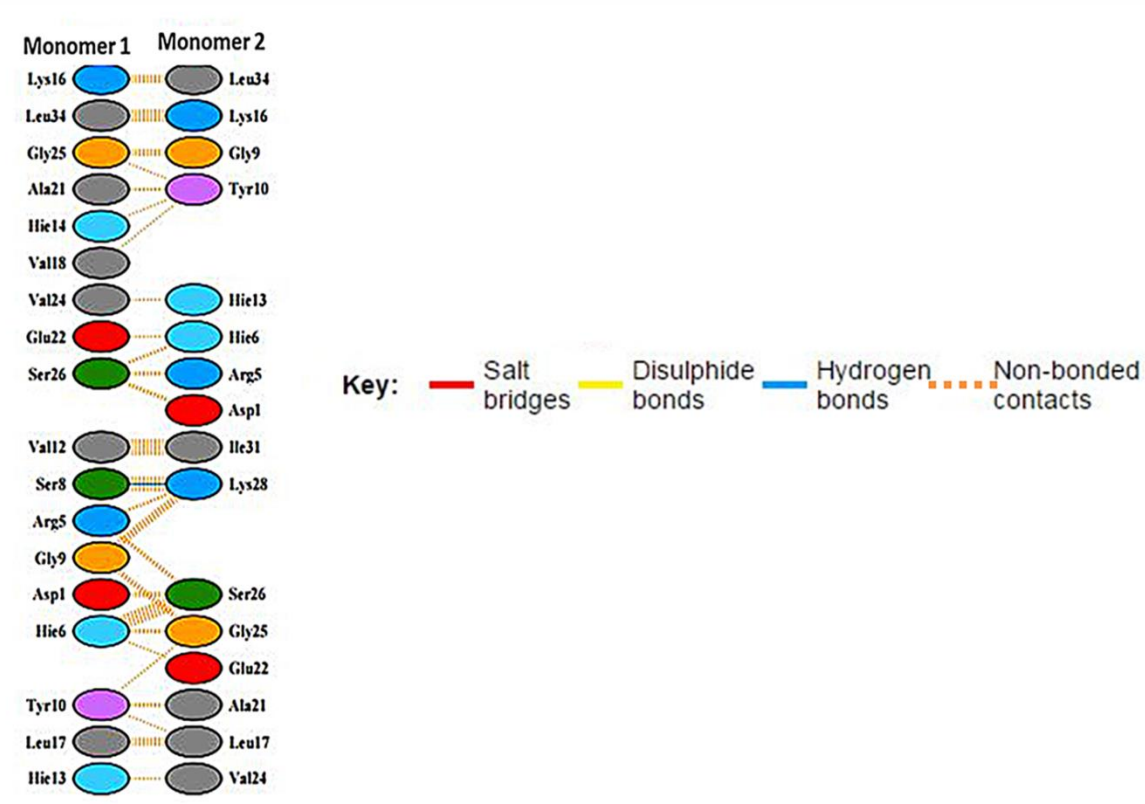

Figure 10.13. *The interface residues of the $A\beta_{1-42}/A\beta_{1-42}$ homo-dimer showing different interactions as predicted by the PDBsum server.*

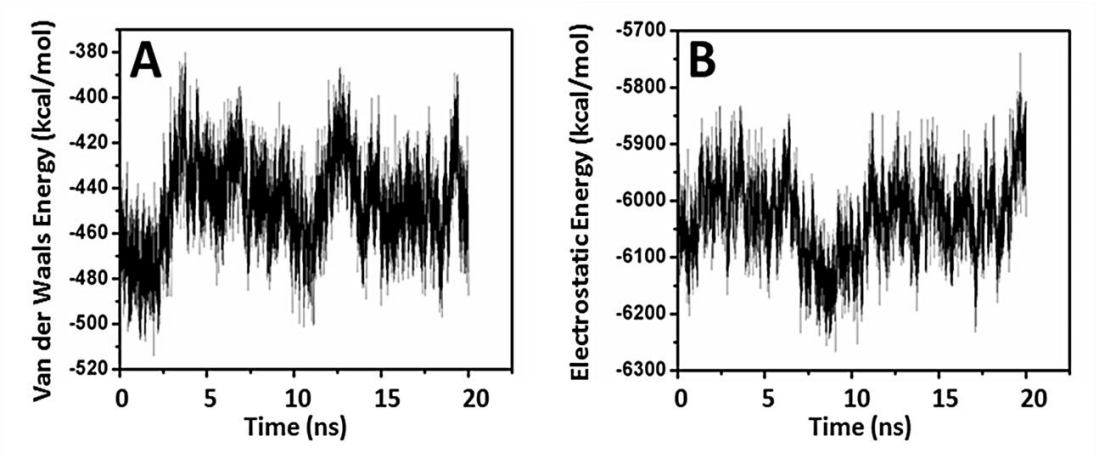

Figure 10.14. *A). VdWaals; B) Electrostatic Energy vs time course of simulation period for the $A\beta_{1-42}/A\beta_{1-40}$ hetero-dimer after MD simulation run at constant inter-chain distance.*

10.4.6. Estimation of binding free energy of $A\beta_{1-40}$ peptide to $A\beta_{1-42}$ peptide by MM-PBSA method:

To evaluate the binding affinity between the two isoforms, binding free energy was calculated using the MM/PBSA approach based on MD simulations. The MM/PBSA binding free energies is summarized in **Table 10.1**. The purpose of the MM/PBSA calculations is to explain the binding affinity difference between the two isoforms. The PBTOT and GBTOT values that indicate the final estimated binding free energy (from the Poisson –Boltzmann (PB) and GB model, respectively) for the $A\beta_{1-42}/A\beta_{1-40}$ hetero-dimer complexes were found to be -41.34 kcal/mol and -39.15 kcal/mol respectively. We found the PBTOT and GBTOT values for the $A\beta_{1-42}/A\beta_{1-42}$ homo-dimer complexes to be -18.62 kcal/mol and -22.92 kcal/, respectively. Averaging over the MD runs we obtained ΔG_{bind} = -78.31 kcal/mol. The binding free energy is negative supporting good binding of $A\beta_{1-40}$ to $A\beta_{1-42}$ peptide. Additionally, we have calculated the ΔG_{bind} of $A\beta_{1-42}/A\beta_{1-42}$ homo-dimer which came of around -45.85 kcal/mol.

Table 10.1: *Binding free energy of $A\beta_{1-40}$ peptide to $A\beta_{1-42}$ peptide in the hetero-dimer system and $A\beta_{1-42}$ to $A\beta_{1-42}$ in the homo-dimer system.*

System	ΔE_{ele} (kcal/mol)	ΔE_{vdW} (kcal/mol)	ΔG_{GB} (kcal/mol)	ΔG_{SA} (kcal/mol)	ΔG_{bind} (kcal/mol)
$A\beta_{1-40}$-$A\beta_{1-42}$	21.95	-66.61	-39.15	5.50	-78.31
$A\beta_{1-42}$-$A\beta_{1-42}$	-11.64	-43.21	-22.92	31.92	-45.85

It thereby appears that different bonding and non-bonding interactions of the $A\beta_{1-40}$ peptide to $A\beta_{1-42}$ peptide are responsible for the co-oligomer formation. Our results also display hetero-dimers with diversified conformations from extended monomeric unit to structures with coils and helices. Similar results on different conformations of Aβ peptide dimers were reported by the atomic-level study of Aβ-dimer formation of Aβ16-22 fragment by Nussinov *et. al.*, where they revealed that the dimers of the aggregation-prone fragment of Aβ peptide may adopt diverse conformations [243].

10.5. Conclusions:

Our results show that hetero-dimer complex of $A\beta_{1-40}$ peptide and $A\beta_{1-42}$ peptide can be formed at a moderate distance with high dissociation energy. This finding is in accordance with the inhibitory mechanism of $A\beta_{1-40}$ peptide on $A\beta_{1-42}$ peptide aggregation, suggesting that the native α-helices of $A\beta_{1-42}$ peptide do not change significantly in the monomeric state in presence of $A\beta_{1-40}$ peptide. The lowest energy structure isolated from the PMF plot at a distance of 13 Å was further studied and from its protein-protein interaction study it can be seen that most of the N-terminal regions of $A\beta_{1-42}$ peptide are involved in the hetero-dimer complex formation. Snapshots obtained so far also show that although the C-terminal region is disordered the N-terminal region retains its α-helix content. It is therefore likely that under suitable conditions $A\beta_{1-42}/A\beta_{1-40}$ aggregates are prevalent. Also since ΔG_{bind} value is negative, we can say that $A\beta_{1-40}$ peptide interferes with the $A\beta_{1-42}$ peptide aggregation through binding mechanism. Thus, any comprehensive therapeutic strategy based on antibodies that bind Aβ peptide may need to take account of the presence of co-oligomers in addition to self-oligomers of Aβ peptide. It can thus be predicted that the protective role of $A\beta_{1-40}$ peptide is associated with a strong binding affinity to $A\beta_{1-42}$ peptide. Moreover, as we have shown that in the presence of the $A\beta_{1-40}$ peptide, specific regions important for fibril formation of $A\beta_{1-42}$ peptide exhibit a high fluctuation as well as the distance between the residues involved in salt bridge formation increases, therefore there is likelihood that $A\beta_{1-40}$ peptide may reduce the toxicity of $A\beta_{1-42}$ peptide by degrading the intermediate toxic oligomers or fibrils of $A\beta_{1-42}$ peptide. This question requires further investigation but our preliminary result on the free energy profile of $A\beta_{1-40}$ peptide and $A\beta_{1-42}$ peptide interaction suggests that $A\beta_{1-40}$ peptide can bind and as well as inhibit the aggregation propensity of $A\beta_{1-42}$ peptide.